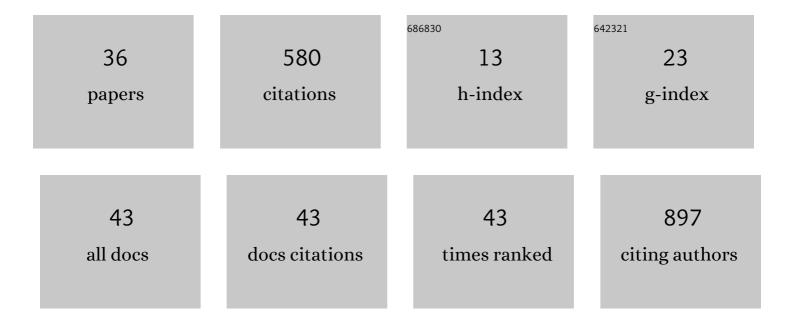
## Ahin Roy

## List of Publications by Year in descending order

Source: https://exaly.com/author-pdf/6948295/publications.pdf Version: 2024-02-01



#	Article	IF	CITATIONS
1	Growth and analysis of the tetragonal (ST12) germanium nanowires. Nanoscale, 2022, 14, 2030-2040.	2.8	3
2	One-Step Grown Carbonaceous Germanium Nanowires and Their Application as Highly Efficient Lithium-Ion Battery Anodes. ACS Applied Energy Materials, 2022, 5, 1922-1932.	2.5	9
3	Liquid phase exfoliation of nonlayered non-van der Waals iron trifluoride (FeF3) into 2D-platelets for high-capacity lithium storing cathodes. FlatChem, 2022, 33, 100360.	2.8	15
4	Covalently interconnected transition metal dichalcogenide networks via defect engineering for high-performance electronic devices. Nature Nanotechnology, 2021, 16, 592-598.	15.6	74
5	Extending the Cyclability of Alkaline Zinc–Air Batteries: Synergistic Roles of Li <sup>+</sup> and K <sup>+</sup> Ions in Electrodics. ACS Applied Materials & Interfaces, 2021, 13, 33112-33122.	4.0	11
6	Characterisation and Defect Analysis of 2D Layered Ternary Chalcogenides. Microscopy and Microanalysis, 2021, 27, 642-643.	0.2	0
7	Postsynthetic treatment of nickel–iron layered double hydroxides for the optimum catalysis of the oxygen evolution reaction. Npj 2D Materials and Applications, 2021, 5, .	3.9	12
8	2D nanosheets from fool's gold by LPE: High performance lithium-ion battery anodes made from stone. FlatChem, 2021, 30, 100295.	2.8	6
9	Charge transport mechanisms in inkjet-printed thin-film transistors based on two-dimensional materials. Nature Electronics, 2021, 4, 893-905.	13.1	52
10	Phase & morphology engineered surface reducibility of MnO2 nano-heterostructures: Implications on catalytic activity towards CO oxidation. Materials Research Bulletin, 2020, 121, 110615.	2.7	27
11	Fluorophosphates as Efficient Bifunctional Electrocatalysts for Metal–Air Batteries. ACS Catalysis, 2020, 10, 43-50.	5.5	29
12	Production of Quasi-2D Platelets of Nonlayered Iron Pyrite (FeS <sub>2</sub> ) by Liquid-Phase Exfoliation for High Performance Battery Electrodes. ACS Nano, 2020, 14, 13418-13432.	7.3	45
13	Morphology Controlled Low-dimensional Single-crystalline SnSe2-graphene Hybrid for near IR Photodetection. Microscopy and Microanalysis, 2020, 26, 2338-2340.	0.2	0
14	Mechanistic Studies of Growth of Ultrathin Pt and Alloy Nanowires. Microscopy and Microanalysis, 2020, 26, 2400-2401.	0.2	0
15	Carrier Dynamics in Ultrathin Gold Nanowires: Role of Auger Processes. Plasmonics, 2020, 15, 1151-1158.	1.8	2
16	Thermal History-Dependent Current Relaxation in hBN/MoS <sub>2</sub> van der Waals Dimers. ACS Nano, 2020, 14, 5909-5916.	7.3	9
17	Polymorphic In-Plane Heterostructures of Monolayer WS <sub>2</sub> for Light-Triggered Field-Effect Transistors. ACS Applied Nano Materials, 2020, 3, 3750-3759.	2.4	5
18	Morphology controlled synthesis of low bandgap SnSe <sub>2</sub> with high photodetectivity. Nanoscale, 2019, 11, 870-877.	2.8	31

Ahin Roy

#	Article	IF	CITATIONS
19	Reduced SrTiO <sub>3</sub> -supported Pt–Cu alloy nanoparticles for preferential oxidation of CO in excess hydrogen. Nanoscale, 2019, 11, 22423-22431.	2.8	13
20	Ba-addition induced enhanced surface reducibility of SrTiO <sub>3</sub> : implications on catalytic aspects. Nanoscale Advances, 2019, 1, 4938-4946.	2.2	7
21	Removal of U(VI) from aqueous solution by adsorption onto synthesized silica and zinc silicate nanotubes: Equilibrium and kinetic aspects with application to real samples. Environmental Nanotechnology, Monitoring and Management, 2018, 10, 127-139.	1.7	8
22	Scalable faceted voids with luminescent enhanced edges in WS <sub>2</sub> monolayers. Nanoscale, 2018, 10, 16321-16331.	2.8	11
23	Manipulation of Optoelectronic Properties and Band Structure Engineering of Ultrathin Te Nanowires by Chemical Adsorption. ACS Applied Materials & Interfaces, 2017, 9, 19462-19469.	4.0	9
24	Nanostructural characterization of artificial pinning centers in PLD-processed REBa2Cu3O7-δfilms. Ultramicroscopy, 2017, 176, 151-160.	0.8	8
25	Negative differential resistance in armchair silicene nanoribbons. Nanotechnology, 2017, 28, 275402.	1.3	6
26	Ambient Dependent Formation of Zn2SiO4 and SiO2 from Core-shell ZnO@SiO2. Microscopy and Microanalysis, 2017, 23, 1758-1759.	0.2	1
27	Wet-chemical Synthesis of Electrochromic WO3 and WxMo1-xO3 Nanomaterials with Phase and Morphology Control. Microscopy and Microanalysis, 2017, 23, 1876-1877.	0.2	0
28	Insights into nucleation, growth and phase selection of WO <sub>3</sub> : morphology control and electrochromic properties. Journal of Materials Chemistry C, 2017, 5, 7307-7316.	2.7	34
29	Ultra-high sensitivity infra-red detection and temperature effects in a graphene–tellurium nanowire binary hybrid. Nanoscale, 2017, 9, 9284-9290.	2.8	31
30	Transmission Electron Microscopic Analysis of One-dimensional Metal Nanowire: The Case of Tellurium and Gold. Materia Japan, 2016, 55, 603-603.	0.1	0
31	Effect of ambient on electrical transport properties of ultra-thin Au nanowires. Applied Physics Letters, 2016, 109, 253108.	1.5	4
32	Synthesis of Hollow Nanotubes of Zn <sub>2</sub> SiO <sub>4</sub> or SiO <sub>2</sub> : Mechanistic Understanding and Uranium Adsorption Behavior. ACS Applied Materials & Interfaces, 2015, 7, 26430-26436.	4.0	39
33	Semiconductor-like Sensitivity in Metallic Ultrathin Gold Nanowire-Based Sensors. Journal of Physical Chemistry C, 2014, 118, 18676-18682.	1.5	17
34	Wrinkling of Atomic Planes in Ultrathin Au Nanowires. Nano Letters, 2014, 14, 4859-4866.	4.5	35
35	Single crystalline ultrathin gold nanowires: Promising nanoscale interconnects. AIP Advances, 2013, 3,	0.6	25
36	Mechanistic Understanding of Formation of Ultrathin Single-Crystalline Pt Nanowires. Journal of Physical Chemistry C, 0, , .	1.5	2